

University of Wollongong  
**Research Online**

---

Faculty of Engineering - Papers (Archive)

Faculty of Engineering and Information  
Sciences

---

1-1-2010

## Scattering of pulsed plane wave from a symmetrical groove doublet configuration

Lan Ding

*University of Wollongong, lding@uow.edu.au*

Jinsong Liu

*Huazhong University of Science and Technology*

Kejia Wang

*Huazhong University of Science and Technology*

Dong Wang

*Huazhong University of Science and Technology*

Follow this and additional works at: <https://ro.uow.edu.au/engpapers>



Part of the [Engineering Commons](#)

<https://ro.uow.edu.au/engpapers/2719>

---

### Recommended Citation

Ding, Lan; Liu, Jinsong; Wang, Kejia; and Wang, Dong: Scattering of pulsed plane wave from a symmetrical groove doublet configuration 2010, 27682-27690.

<https://ro.uow.edu.au/engpapers/2719>

Research Online is the open access institutional repository for the University of Wollongong. For further information contact the UOW Library: [research-pubs@uow.edu.au](mailto:research-pubs@uow.edu.au)

# Scattering of pulsed plane wave from a symmetrical groove doublet configuration

Lan Ding, Jinsong Liu,\* Dong Wang, and Kejia Wang

Wuhan National Laboratory for Optoelectronics, School of Optoelectronic Science and Engineering, Huazhong University of Science and Technology, Wuhan 430074, China

\*jsliu4508@vip.sina.com

**Abstract:** We have provided theoretical study on the spectral and temporal properties of the scattering of pulsed plane wave from a symmetrical groove doublet configuration. Based on the numerical calculation results, we show that the spectrum and the waveform of the scattered field are sensitive to the shape of the rectangular grooves when the grooves are deep enough. In both spectral and temporal domain, a damped oscillatory behavior occurs when the groove spacing increases. Furthermore, the spectral and temporal dependences of the angular distribution are consisted of interference-like fringe patterns. These patterns are sensitive to the size of the groove width and spacing rather than the groove shape when the depth is small enough. Our study takes the analysis of pulse scattering by finite grooves a step further on the theoretical side, and offers opportunities for the control of spectral and temporal properties of pulsed scattered wave in low frequency regime such as THz and microwave domain.

©2010 Optical Society of America

**OCIS codes:** (290.5880) Scattering, rough surfaces; (050.2770) Gratings; (040.2235) Far infrared or terahertz.

---

## References and links

1. K. Barkeshli, and J. L. Volakis, "TE scattering by a two-dimensional groove in a ground plane using higher order boundary conditions," *IEEE Trans. Antenn. Propag.* **38**(9), 1421–1428 (1990).
2. K. W. Whites, E. Michielssen, and R. Mittra, "Approximating the scattering by a material-filled 2-D trough in an infinite plane using the impedance boundary condition," *IEEE Trans. Antenn. Propag.* **41**(2), 146–153 (1993).
3. M. G. Moharam, E. B. Grann, D. A. Pommet, and T. K. Gaylord, "Formulation for stable and efficient implementation of the rigorous coupled-wave analysis of binary gratings," *J. Opt. Soc. Am. A* **12**(5), 1068–1076 (1995).
4. A. A. Maradudin, A. V. Shchegrov, and T. A. Leskova, "Resonant scattering of electromagnetic waves from a rectangular groove on a perfectly conducting surface," *Opt. Commun.* **135**(4-6), 352–360 (1997).
5. M. A. Morgan, and F. K. Schwering, "Mode expansion solution for scattering by a material filled rectangular groove," *Prog. Electromagn. Res. PIER* **18**, 1–17 (1998).
6. G. Bao, and W. Zhang, "An Improved Mode-Matching Method for Large Cavities," *IEEE Antennas Wirel. Propag. Lett.* **4**(1), 393–396 (2005).
7. G. Lévêque, O. J. F. Martin, and J. Weiner, "Transient behavior of surface plasmon polaritons scattered at a subwavelength groove," *Phys. Rev. B* **76**(15), 155418 (2007).
8. R. A. Depine, and D. C. Skigin, "Scattering from metallic surfaces having a finite number of rectangular grooves," *J. Opt. Soc. Am. A* **11**(11), 2844–2850 (1994).
9. N. C. Bruce, "Control of the backscattered intensity in random rectangular-groove surfaces with variations in the groove depth," *Appl. Opt.* **44**(5), 784–791 (2005).
10. X. Y. Yang, H. T. Liu, and P. Lalanne, "Cross Conversion between Surface Plasmon Polaritons and Quasicylindrical Waves," *Phys. Rev. Lett.* **102**(15), 153903 (2009).
11. P. Lalanne, J. P. Hugonin, H. T. Liu, and B. Wang, "A microscopic view of the electromagnetic properties of sub- $\lambda$  metallic surfaces," *Surf. Sci. Rep.* **64**(10), 453–469 (2009).
12. M. A. Basha, S. Chaudhuri, and S. Safavi-Naeini, "A study of coupling interactions in finite arbitrarily-shaped grooves in electromagnetic scattering problem," *Opt. Express* **18**(3), 2743–2752 (2010).
13. L. Ding, J. S. Liu, D. Wang, and K. J. Wang, "Coupling interaction of electromagnetic wave in a groove doublet configuration," *Opt. Express* **18**(20), 21083–21089 (2010).
14. H. Cao, A. Agrawal, and A. Nahata, "Controlling the transmission resonance lineshape of a single subwavelength aperture," *Opt. Express* **13**(3), 763–769 (2005).
15. A. Agrawal, H. Cao, and A. Nahata, "Time-domain analysis of enhanced transmission through a single subwavelength aperture," *Opt. Express* **13**(9), 3535–3542 (2005).

16. A. Agrawal, H. Cao, and A. Nahata, "Excitation and scattering of surface plasmon-polaritons on structured metal films and their application to pulse shaping and enhanced transmission," *N. J. Phys.* **7**, 249 (2005).
  17. J. B. Pendry, L. Martin-Moreno, and F. J. Garcia-Vidal, "Mimicking Surface Plasmons with Structured Surfaces," *Science* **305**(5685), 847–848 (2004).
  18. F. J. Garcia-Vidal, L. Martin-Moreno, and J. B. Pendry, "Surfaces with holes in them: New plasmonic metamaterials," *J. Opt. A* **7**, S97–S101 (2005).
  19. Q. Gan, Z. Fu, Y. Ding, and F. Bartoli, "Introduction, Ultrawide-Bandwidth Slow-Light System Based on THz Plasmonic Graded Metallic Grating Structures," *Phys. Rev. Lett.* **100**(25), 256803 (2008).
  20. J. A. Sánchez-Gil, and A. A. Maradudin, "Dynamic near-field calculations of surface-plasmon polariton pulses resonantly scattered at sub-micron metal defects," *Opt. Express* **12**, 883–894 (2004).
- 

## 1. Introduction

Although the scattering of electromagnetic wave on a finite collection of grooves has been extensively studied over the last several decades, there appears to be resurgent interest in this topic. This is driven largely by the ongoing desire to understand the underlying physics and develop new applications of wave manipulation. There have been several studies of the scattering of electromagnetic waves by isolated grooves of various types on an otherwise planar metal surface [1–7], as well as studies of scattering processes in multi-groove configurations [8–13]. However, in all of this work the incident wave was assumed as continuous wave, *i.e.* the incident wave was assumed to be monochromatic. Recent experimental time-domain studies on the transmission of pulsed THz wave through a single aperture surrounded by annular grooves have been reported [14–16], demonstrating the ability to alter the pulse shape of transmitted waveform using such a structure. These time-domain studies are very useful, since they could be applied to controlling arbitrarily the spectral and temporal properties of pulsed wave, which is of fundamental importance for the study of optical physics, and has practical significance for applications [16]. On the theoretical side, the scattering of THz pulse from grooves plays an important role for this phenomenon. To our knowledge, the pulse scattering from multi-groove configurations contains two important processes: One is the coupling interaction between grooves. The other is the interference between the fields scattered by each of the grooves. Therefore, the scattering of pulsed wave from two grooves, namely groove doublet configuration, is the simplest situation. However, even in this basic case, little is known on the spectral and temporal characteristics of the pulse scattering by grooves.

By the use of the waveguide mode (WGM) method, coupling interaction of monochromatic electromagnetic wave in a groove doublet configuration was studied [13]. On this basis, in this paper, we provide a quantitatively study on the characteristics of the scattering of pulsed plane wave from a symmetrical groove doublet configuration. Numerical calculations of the spectral and temporal scattered field amplitudes are carried out for varying groove shape, spacing, and scattering angle. Based on the results, we show that the shift of the spectral maximum and the division of the spectrum can be obtained at certain values of configuration parameters, as well as the broadening and splitting behavior of the pulse in time domain. The spectrum and waveform of the scattered field are sensitive to the shape of the rectangular grooves when the grooves are deep enough. In both spectral and temporal domain, a damped oscillatory behavior occurs with increasing groove spacing. Furthermore, the spectral and temporal dependences of the angular distribution are consisted of interference-like fringe patterns. These patterns are relatively insensitive to the groove shape when the groove depth is small enough. Through engineering of the geometrical parameters of the groove doublet configuration, we are able to control the spectral and temporal properties of the pulsed scattered wave in low frequency regime such as THz and microwave domain. We believe that new applications such as pulse shaping antennas, and couplers could be designed based on our study.

## 2. Problem formulation

In this section, through the waveguide mode (WGM) method with coupling interaction [13], we explore the time-dependent total scattered field of a symmetrical groove doublet

configuration. For simplicity, we assume that the configuration consists of two rectangular grooves in a perfect-conductor surface (PCS), as shown in Fig. 1. A pulsed transverse magnetic (TM) plane wave ( $\mathbf{E}_i = E_x \hat{x} + E_z \hat{z}$ , and  $\mathbf{H}_i = H_y \hat{y}$ ) is obliquely incident upon the configuration at an arbitrary angle of incidence  $\theta_i$ . As discussed in our previous work [13], the compound scattered field of each groove ( $\mathbf{H}_{1S}^{com}$ ,  $\mathbf{H}_{2S}^{com}$ ) consists of two parts: the basic scattered field ( $\mathbf{H}_{1S}$ ,  $\mathbf{H}_{2S}$ ) generated directly by  $\mathbf{H}_i$ , and the additional scattered field ( $\mathbf{H}'_{1S}$ ,  $\mathbf{H}'_{2S}$ ) generated through coupling interaction, as illustrated in Fig. 1. Therefore, the total scattered field of the groove doublet configuration can be obtained as  $\mathbf{H}_S^{total} = \mathbf{H}_{1S}^{com} + \mathbf{H}_{2S}^{com}$ .

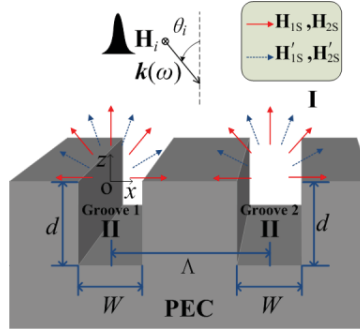


Fig. 1. Scattering by a groove doublet configuration in a perfect electrical conductor (PEC) plane, including the geometrical parameters  $W$ ,  $d$ , and  $\Lambda$ . A pulsed plane TM wave is incident upon the configuration, with the angle of incidence  $\theta_i$ . The groove doublet configuration is in vacuum, thus  $\epsilon_{rI} = \epsilon_{rII} = 1$ , and  $\mu_{rI} = \mu_{rII} = 1$ .

We assume that the incident pulse is characterized by its only non-zero component of the magnetic field in vacuum,

$$\mathbf{H}_i(x, z; \tau) = \hat{y} \cdot \int_{-\infty}^{+\infty} d\omega H_0(\omega) \exp[-ik(\omega)(x \sin \theta_i - z \cos \theta_i)] \exp(i\omega\tau), \quad (1a)$$

$$H_0(\omega) = \exp[-(\omega - \omega_0)^2 / (\Delta\omega)^2] / (\sqrt{\pi}\Delta\omega), \quad (1b)$$

where  $\tau$  is the relative time,  $H_0(\omega)$  is a Gaussian spectral amplitude, and  $k(\omega)$  is the incident wave vector in free space. If the groove doublet configuration is in vacuum, according to [5,13], the time-dependent basic scattered field of each groove can be deduced as

$$\mathbf{H}_{jS}(\rho_j, \theta_j; \tau) = \hat{y} \cdot \int_{-\infty}^{+\infty} d\omega H_{jS}(\rho_j, \theta_j; \omega) \exp(i\omega\tau), \quad (2a)$$

$$H_{jS}(\rho_j, \theta_j; \omega) \approx H_0(\omega) W \sqrt{\frac{ik(\omega)}{2\pi\rho_j}} \exp[-ik(\omega)\rho_j] \sum_{n_j=0}^{N(\omega)} c_{jn_j}(\omega) L_{jn_j}(\theta_j, \omega), \quad (2b)$$

in which  $j = 1, 2$  represent groove 1 and 2, respectively,  $\theta_j$  is the scattering angle,  $c_{jn_j}(\omega)$  is the field expansion coefficients, and  $L_{jn_j}(\theta_j, \omega)$  represents far-field Fourier integration of modal aperture field. Then the time-dependent additional scattered field of each groove generated through coupling interaction can be obtained as

$$\mathbf{H}'_{jS}(\rho_j, \theta_j; \tau) = \hat{y} \cdot \int_{-\infty}^{+\infty} d\omega H'_{jS}(\rho_j, \theta_j; \omega) \exp(i\omega\tau), \quad (3a)$$

$$H'_{jS}(\rho_j, \theta_j; \omega) \approx H'_j(\omega)W \sqrt{\frac{ik(\omega)}{2\pi\rho_j}} e^{-ik(\omega)\rho_j} \sum_{n_j=0}^{N(\omega)} c'_{jn_j}(\omega) L_{jn_j}(\theta_j, \omega), \quad (3b)$$

where  $c'_{jn_j}(\omega)$  is the additional field expansion coefficients. Note that a series truncation of  $N(\omega) = 2W/\lambda$ , which provides excellent results in [5] and [13], has been used in this article.

As mentioned above, the compound scattered field of each groove consists of the basic scattered field and the additional scattered field. Therefore, the compound far-zone scattered fields can be represented as

$$\mathbf{H}_{1S}^{com}(\rho_1, \theta_1; \tau) = \mathbf{H}_{1S}(\rho_1, \theta_1; \tau) + \mathbf{H}'_{1S}(\rho_1, \theta_1; \tau), \quad (4)$$

$$\mathbf{H}_{2S}^{com}(\rho_2, \theta_2; \tau) = \mathbf{H}_{2S}(\rho_2, \theta_2; \tau) + \mathbf{H}'_{2S}(\rho_2, \theta_2; \tau). \quad (5)$$

It should be noted that the polar coordinate origin of Eq. (4) is set at  $(x = 0, z = 0)$ , while that of Eq. (5) is set at  $(x = \Lambda, z = 0)$ . The compound scattered fields of groove 1 and 2 can be investigated by Eq. (4) and (5), respectively. Then, by using of coordinate transformation and vector addition, the time-dependent total scattered field of the groove doublet configuration can be expressed as

$$\mathbf{H}_S^{total}(\rho_1, \theta_1; \tau) = \mathbf{H}_{1S}^{com}(\rho_1, \theta_1; \tau) + \mathbf{H}_{2S}^{com}(\rho_2(\rho_1, \theta_1), \theta_2(\rho_1, \theta_1); \tau). \quad (6)$$

In Eq. (6), the process of coordinate transformation has the form

$$\begin{cases} \rho_2(\rho_1, \theta_1) = \sqrt{\rho_1^2 + \Lambda^2 - 2\Lambda\rho_1 \sin \theta_1} \\ \theta_2(\rho_1, \theta_1) = \arctan\left(\tan \theta_1 - \frac{\Lambda}{\rho_1 \cos \theta_1}\right) \end{cases}. \quad (7)$$

According to Eq. (4) to (7), the properties of scattering of a pulsed plane wave from a groove doublet configuration can be analyzed thoroughly. Although the case of two grooves is discussed for simplicity in this article, the formulation developed here can be generalized to arbitrary number of grooves, which is similar to the process introduced in [13] for monochromatic incident wave.

### 3. Numerical results and discussion

In order to discuss the spectral and temporal properties of the scattering of a Gaussian pulse from the two grooves, we now calculate the total scattered field by the formulation in section 2. In practice, grooves are usually fabricated on metallic surfaces, which are treated as PCSs in THz domain [17–19]. Thus we consider an incident pulse with  $\omega_0 = 2\pi f_0$  ( $f_0 = 1$  THz) and spectral width  $\Delta\omega/\omega_0 = 0.1$  (FWHM~5 ps). The spectrum and waveform of the incident pulse are shown in Fig. 2(a) and (b), in which the spectral amplitude has been normalized to 1. To make the numerical results clear, all size parameters of the grooves are compared with the central wavelength  $\lambda_0$  ( $\lambda_0 = 300 \mu\text{m}$ ), and the angle of incidence  $\theta_i$  is fixed to 0. Moreover, a cylindrical surface of observation, whose radius is fixed to  $\rho_0 = 400\lambda_0$  ( $\rho_0 \gg \Lambda > W$ ), has been defined as shown in Fig. 2(c). Since the cylindrical surface of observation is in the far-field region, the scattered field at the surface can be calculated through Eq. (6). The shape of both grooves is expressed as the ratio of the groove width to depth. We designate this ratio by  $\delta = W/d$ . Numerical calculations of the spectral and temporal scattered field amplitudes are carried out for varying groove shape ( $\delta$ ), spacing ( $\Lambda$ ), and scattering angle ( $\theta_1$ ).

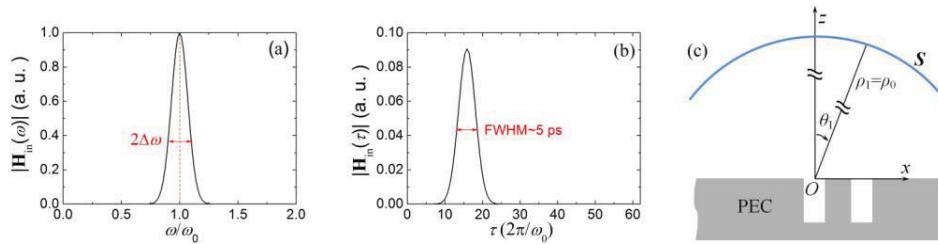


Fig. 2. The (a) spectral and (b) temporal dependences of the incident Gaussian pulse with  $\omega_0 = 2\pi f_0$  ( $f_0 = 1$  THz) and spectral width  $\Delta\omega/\omega_0 = 0.1$  (FWHM~5 ps). The spectral amplitude has been normalized to 1. (c) The cylindrical surface of observation is defined as  $S$  with a fixed radius of  $\rho_0 = 400\lambda_0$ .

Results of the  $\delta$  dependence of the spectral scattered field amplitude are shown in Fig. 3(a) and (c). In the range of  $\delta < \delta_0$ , the spectrum of the scattered field varies drastically with  $\delta$ , and divides into two or more parts at some certain values of  $\delta$ . When  $\delta$  exceeds  $\delta_0$ , the spectral change of the scattered field is relatively smooth. In both cases, the shift of the spectral maximum can be observed, which is caused only by the distortion of the spectral shape rather than by any nonlinear effect. The time-domain results corresponding to Fig. 3(a) and (c) are shown in Fig. 3(b) and (d), respectively. It should be noted again that the horizontal axis  $\tau$  for all time-domain waveforms is the relative time. When  $\delta$  is smaller than  $\delta_0$ , the waveform of the scattered field changes drastically with  $\delta$ . The pulse broadens and even splits into two or more pulses at certain values of  $\delta$ . As  $\delta$  exceeds  $\delta_0$ , the time-domain field amplitude varies smoothly. In our discussion,  $\delta_0$  is an important parameter. For the case of  $W = 0.5\lambda_0$ ,  $\delta_0$  is about 1 while that of  $W = 1.5\lambda_0$  is 3.

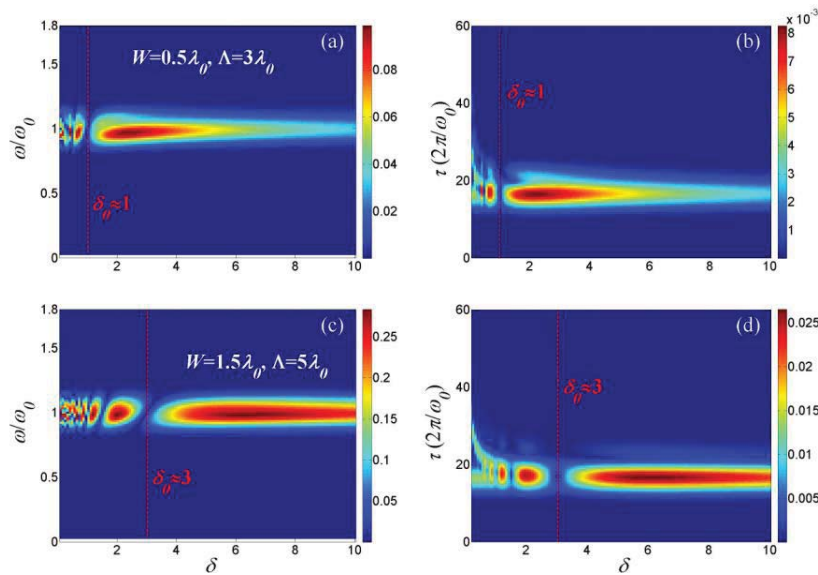


Fig. 3. The  $\delta$  dependences of the (a) spectral and (b) temporal scattered field amplitudes for  $W = 0.5\lambda_0$ ,  $\Lambda = 3\lambda_0$ , and the (c) spectral and (d) temporal results for  $W = 1.5\lambda_0$ ,  $\Lambda = 5\lambda_0$ . The scattering angle is fixed to  $0^\circ$  in the calculation.

We have also calculated the  $\delta$  dependence of scattered field amplitude for different groove widths (not displayed here), and found that  $\delta_0$  can be estimated by  $\delta_0 \approx W/0.5\lambda_0$  for any case of  $W$ , which corresponds to a groove depth ( $d$ ) of about  $0.5\lambda_0$ . When  $\delta$  is smaller than  $\delta_0$ , some minima of field can be seen in these calculation results, which are due to the groove resonance of guided modes. In other word,  $\delta = \delta_0$  (or  $d = 0.5\lambda_0$ ) is the fundamental resonance condition. Actually, since the surface is treated as PCS, the resonance is determined only by the groove

depth  $d$  rather than the width  $W$ . Therefore, we have also shown the  $d$  dependence of scattered field amplitude for the central frequency  $\omega_0$  in Fig. 4(a). The period of the resonance can be obtained as  $0.5\lambda_0$  from Fig. 4(a).

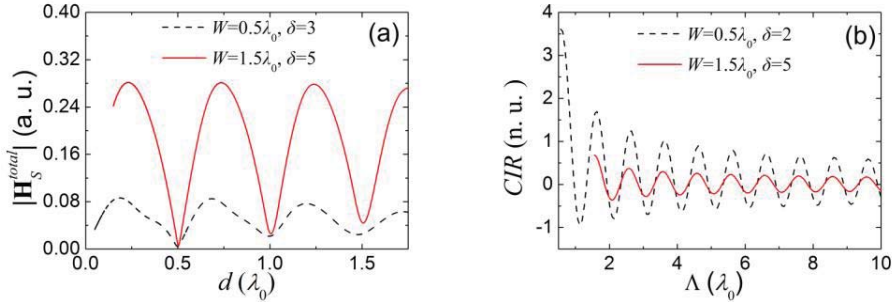


Fig. 4. The  $d$  dependence of the total scattered field amplitude (a) corresponding to the central frequency in Fig. 3. The  $\Lambda$  dependence of  $CIR$  (b) corresponding to the central frequency in Fig. 5. The scattering angle is fixed to  $0^\circ$  in the calculation.

Figure 5(a) and (c) show the groove spacing ( $\Lambda$ ) dependence of the spectral scattered field amplitude. A damped oscillatory behavior with period of about  $\lambda_0$  can be observed clearly for given frequency, which is similar to the case of monochromatic incident wave [13]. The damped oscillations of scattered field are due to the same behavior of coupling interaction between the two grooves. As shown in Fig. 4(b), the coupling interaction can be investigated quantitatively through *coupling interaction ratio* ( $CIR$ ) [13] for given frequency. These oscillations come from interference between  $\mathbf{H}_{1S}^{com}$  and  $\mathbf{H}_{2S}^{com}$ . Meanwhile, the damped behavior with increasing  $\Lambda$  is attributed to the decreasing of the coupling interaction between grooves, as shown in Fig. 4(b). The quasi-periodic shifts of the spectral maximum can also be observed, and the spectrum divides into two or more parts at some certain values of  $\Lambda$ , as shown in Fig. 5(a) and (c). The temporal scattered field amplitudes versus  $\Lambda$  are illustrated in Fig. 5(b) and (d). The pulse broadens and even splits at certain values of  $\Lambda$ , and these two behaviors are more and more obvious with increasing  $\Lambda$ . One can also see from Fig. 5(b) and (d) that a damped oscillatory behavior with period of about  $\lambda_0$  occurs in the main pulse. This behavior corresponds to that of spectral, and its mechanism has been discussed above.

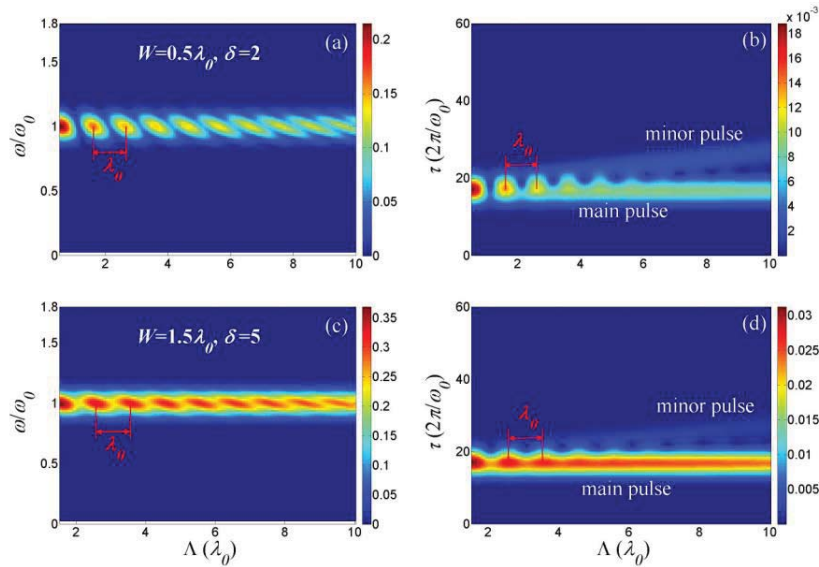


Fig. 5. The  $\Lambda$  dependences of the (a) spectral and (b) temporal scattered field amplitudes for  $W = 0.5\lambda_0$ ,  $\delta = 2$ , and the (c) spectral and (d) temporal results for  $W = 1.5\lambda_0$ ,  $\delta = 5$ . The scattering angle is fixed to  $0^\circ$  in the calculation.

The spectral dependence of the scattering angular distribution is shown in Fig. 6(a), (c), (e), and (g). These angular distributions, which consist of interference-like fringe patterns, are symmetrical about  $\theta_1 = 0^\circ$  with spectral distortion. Such distortion differs from one scattering angle to another. Different from the case of spectral, the angular fringe pattern associated with time domain is distorted along its time evolution drastically, thus leading to asymmetry in the angular distribution, as shown in Fig. 6(b), (d), (f), and (h). It is obvious that all these angular fringe patterns come from the interference between the two scattered fields  $\mathbf{H}_{1S}^{com}$  and  $\mathbf{H}_{2S}^{com}$ . One can also see from these figures that both spectral and temporal dependences of the angular distribution are not sensitive to  $\delta$  for the case of  $d < 0.5\lambda_0$ , but they are sensitive to  $W$  and  $\Lambda$ . It means that these distributions are sensitive to the size of the groove width and spacing rather than the groove shape when  $d < 0.5\lambda_0$ .

These numerical studies indicate that the scattering of pulsed plane wave from a groove doublet configuration could be conveniently analyzed by the formulation developed in part 2. Meanwhile, the results obtained above could be applied to controlling the spectral and temporal properties of pulsed wave, which is important in a broad range of applications, such as pulse shaping.

Since the two grooves are assumed to be fabricated on PCSs, our results are applicable for metallic configurations in low frequency regime such as THz and microwave domain. It should be noted that this is not very rigorous in case the groove width is very narrow because the finite permittivity of metals will affect the results. However, for metals in low frequency regime, PEC approximation leads to simple analytical expressions of many kinds of models even for subwavelength structures [5,13,17–19]. Moreover, when the surface plasmon polaritons (SPPs) are stimulated by incident wave on the structured metallic surface under some conditions, the scattering properties of pulsed wave will be different [20].



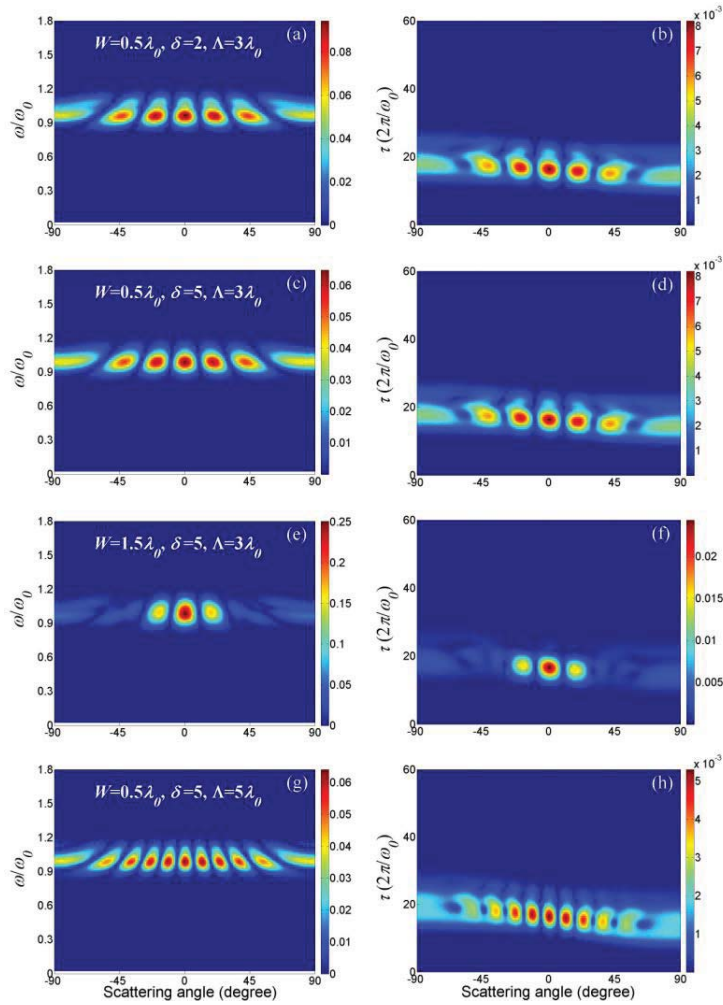


Fig. 6. The spectral dependence of the angular distribution for (a)  $W = 0.5\lambda_0$ ,  $\delta = 2$ , and  $\Lambda = 3\lambda_0$ , (c)  $W = 0.5\lambda_0$ ,  $\delta = 5$ , and  $\Lambda = 3\lambda_0$ , (e)  $W = 1.5\lambda_0$ ,  $\delta = 5$ , and  $\Lambda = 3\lambda_0$ , and (g)  $W = 0.5\lambda_0$ ,  $\delta = 5$ , and  $\Lambda = 5\lambda_0$ . Meanwhile, (b), (d), (f), and (h) are the temporal results corresponding to (a), (c), (e), and (g), respectively.

#### 4. Conclusion

In conclusion, we have quantitatively studied the spectral and temporal properties of the scattering of pulsed plane wave from a symmetrical groove doublet configuration. The formulation of scattering of monochromatic waves from two grooves has been extended to pulsed waves. Numerical simulations of the spectral and temporal scattered field amplitudes have been carried out for varying  $\delta$ ,  $\Lambda$ , and  $\theta_1$ . Results show that the shift of the spectral maximum and the division of the spectrum can be obtained at certain values of geometrical parameters, as well as the broadening and splitting behavior of the scattered pulse in time domain. The spectrum and the waveform of the scattered field are sensitive to the groove shape ( $\delta$ ) when  $d$  is greater than  $0.5\lambda_0$ . In both spectral and temporal domain, a damped oscillatory behavior with period of about  $\lambda_0$  occurs with increasing groove spacing. Moreover, the spectral and temporal dependences of the angular distribution are consisted of interference-like fringe patterns. These patterns are sensitive to the size of the groove width and spacing rather than the groove shape when  $d$  is smaller than  $0.5\lambda_0$ . Although a

symmetrical groove doublet configuration is discussed here for simplicity, we believe that the formulation could be as well generalized to the case of asymmetric double grooves.

Finally, our study takes the analysis of pulse scattering by finite grooves a step further on the theoretical side. Through these results, we are able to control the spectral and temporal properties of pulsed scattered wave in low frequency regime such as THz and microwave domain. More applications such as pulse shaping antennas, and couplers could be designed based upon the results obtained in this paper.

### **Acknowledgments**

The National Natural Science Foundation of China under grant No. 10974063, the Research Foundation of Wuhan National Laboratory under Grant No. P080008, and the Foundation Research Funds for the Central Universities under Grant No. 2010MS041 have supported this research.